

# Densification of zirconia-containing sialon composites by $\text{Sm}_2\text{O}_3$

Y. -B. CHENG

*Department of Materials Engineering, Monash University, Melbourne, Victoria 3168, Australia*

D. P. THOMPSON

*Materials Division, Department of Mechanical, Materials and Manufacturing Engineering, University of Newcastle upon Tyne, UK*

$\text{Sm}_2\text{O}_3$  was used as an additive for  $\text{ZrO}_2/\text{O}'$ -sialon composites and showed remarkably good densification behaviour on sintering.  $\text{Sm}_2\text{O}_3$  appeared to behave as a densification rather than a stabilization additive and the low eutectic temperature in this system facilitated densification before zircon dissociation. An important advantage is that the final sintering temperature is then determined by the minimum temperature at which full conversion from  $\alpha$ - $\text{Si}_3\text{N}_4$  to  $\text{O}'$ -sialon can be achieved. At this temperature (1500–1550 °C), grain growth of zirconia is minimal, and this allows control of small grain size for the zirconia particles.

## 1. Introduction

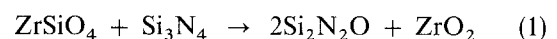
To increase the fracture toughness of non-oxide ceramics, various types of particulate dispersions have been introduced into non-oxide matrices in an attempt to introduce different fracture-energy absorption mechanisms into these materials. In particular, the benefits of incorporating  $\text{ZrO}_2$  particles into  $\text{Si}_3\text{N}_4/\text{Si}_2\text{N}_2\text{O}$  matrix composites have received detailed attention [1]. It has been reported that the stoichiometric reaction between  $\text{ZrSiO}_4$  and  $\text{Si}_3\text{N}_4$  at about 1700 °C can result in the formation of a zirconia-sialon composite containing 23 vol % zirconia and 77 vol % of  $\text{O}'$ -sialon phases [2]. The incorporation of transformable zirconia into the sialon matrix offers the possibility of toughening the composites by a more economical process. In the early work in this field,  $\text{Y}_2\text{O}_3$  was used as an additive in the starting compositions. Although  $\text{Y}_2\text{O}_3$  is effective in both stabilizing the zirconia and densifying the composites, it is not easy to select an optimum amount of a single oxide additive to balance these two requirements simultaneously. With low  $\text{Y}_2\text{O}_3$  additions, the full densification of the material was a problem; whereas adding more  $\text{Y}_2\text{O}_3$  to achieve better densification resulted in the zirconia being stabilized into non-transformable  $t'$  or cubic forms [2]. As a result, no fracture-toughness improvement was experienced in the composites.

It is obvious that the dual function of  $\text{Y}_2\text{O}_3$  in these materials produces complications because the competition for the  $\text{Y}_2\text{O}_3$  between the liquid phase and the zirconia is not dependent on a single factor. Our previous research on zirconia/glass-ceramic composites showed that zirconia stabilization can be more accurately controlled by adding  $\text{Y}_2\text{O}_3$  plus another additive which can assist densification [3]. The process would be ideal if the composite sintered to the

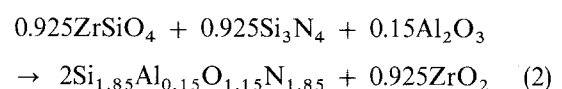
theoretical density and exhibited high toughness and strength, i.e. the particle size of the  $\text{Si}_2\text{N}_2\text{O}$  grains was small, and the transient liquid phase involved in densification had been completely converted to silicon oxynitride leaving a negligible residual-grain-boundary glassy phase. Also it would be desirable to retain transformable tetragonal zirconia of optimum particle size ( $< 1 \mu\text{m}$ ) in the composite [4]. For a further study on the processing of the zirconia/ $\text{O}'$ -sialon composites, a series of combinations involving  $\text{Y}_2\text{O}_3$  plus other additives (such as  $\text{Sm}_2\text{O}_3$ ,  $\text{CaO}$  and  $\text{MgO}$ ) have been used. In this paper, the role of  $\text{Sm}_2\text{O}_3$  in densification and zirconia stabilization is discussed. The advantage of using rare-earth additions (e.g.  $\text{Sm}_2\text{O}_3$ ) for nitrogen ceramics is that they offer high nitrogen content and hence improved refractoriness of the residual-grain-boundary glassy phase. Moreover, due to the large atomic weight of rare-earth oxides, about 8 w/o of  $\text{Sm}_2\text{O}_3$  is equivalent to the same number of moles as 1 w/o  $\text{MgO}$  which therefore represents a very small amount of densifying additive.

## 2. Experimental procedure

The fundamental equation describing the formation of  $\text{ZrO}_2$  toughened  $\text{O}'$ -sialons is:



which in principle could give a fine dispersion of zirconia ( $\sim 23$  vol %) in a matrix of silicon oxynitride (O phase). With the addition of  $\text{Al}_2\text{O}_3$  into the composition, an  $\text{O}'$ -sialon of composition  $\text{Si}_{2-x}\text{Al}_x\text{O}_{1+x}\text{N}_{2-x}$  is formed. The following reaction was used to produce a composite containing both zirconia and  $\text{O}'$ -sialon with  $x = 0.15$ ,



In this paper the starting mix involved in Reaction 2 is referred to as composition Z-23.

For studying the densification behaviour of  $\text{Sm}_2\text{O}_3$ , varying amounts of  $\text{Sm}_2\text{O}_3$  were added to the basic composition (Z-23) as shown in Table I. A series of sintering runs in the temperature range 1300–1700 °C was carried out in order to understand the mechanism of densification and the reaction sequence. Sintering was carried out in a carbon resistance furnace. Bulk densities of fired pellets were determined using the water-immersion technique. All specimens were boiled in water for half an hour prior to density measurement. Hardness and fracture toughness were measured by indentation using a 10 kg load [5]. Phase identification was carried out by X-ray diffraction (XRD) using both a Hägg-Guinier focusing camera and an X-ray diffractometer. Microstructures were

observed by scanning electron microscopy (SEM, using a JSM35 instrument) and transmission electron microscopy (TEM, with a JEOL 100C instrument). More experimental details can be found elsewhere [2].

### 3. Results and discussion

#### 3.1. Reaction sequence

The crystalline phases determined from the samples sintered at different temperatures for 1 hour, are shown in Table II. It was found that the O' phase started to form at 1500 °C and the reaction between  $\text{ZrSiO}_4$  and  $\text{Si}_3\text{N}_4$  was complete at 1550 °C. The trace amount of residual  $\alpha\text{-Si}_3\text{N}_4$  could be eliminated at 1550 °C with a longer soaking period. The reaction sequence corresponding to the formation of an O'-ZrO<sub>2</sub> composite is shown in Fig. 1, as determined from X-ray results. Comparing this sequence with that of single phase O'-sialon material densified with  $\text{Y}_2\text{O}_3$  [6] and of O'-ZrO<sub>2</sub>-Y<sub>2</sub>O<sub>3</sub> mixtures [7], temperatures of both densification and completion of O' formation are much lower for the present material. For example, the complete conversion to O' in the  $\text{Sm}_2\text{O}_3$ -containing system takes place about 100 °C lower than the results given in [6, 7]; this greatly benefits the control of particle size in this material.

$\text{Sm}_2\text{O}_3$  did not stabilize zirconia unless a very high ratio of  $\text{Sm}_2\text{O}_3$  to  $\text{ZrO}_2$  was employed. Even when the starting  $\text{Sm}_2\text{O}_3$ : $\text{ZrO}_2$  ratio was as high as 23.5 wt %

TABLE I Starting compositions

Sample	Compositions	$\text{Sm}_2\text{O}_3/\text{ZrO}_2$ (wt%)
E	Z-23	0
E1	Z-23 + 1 wt % $\text{Sm}_2\text{O}_3$	2.7
E2	Z-23 + 2 wt % $\text{Sm}_2\text{O}_3$	5.3
E3	Z-23 + 3 wt % $\text{Sm}_2\text{O}_3$	7.8
E4	Z-23 + 6 wt % $\text{Sm}_2\text{O}_3$	15.0
E5	Z-23 + 10 wt % $\text{Sm}_2\text{O}_3$	23.5

TABLE II Crystalline phases determined by X-ray diffractometry at different temperatures: (a) 1300 °C/1h, (b) 1400 °C/1h, (c) 1500 °C/1h, (d) 1550 °C/1h, (e) 1600 °C/1h, and (f) 1700 °C/1h;  $\alpha$  is  $\alpha\text{-Si}_3\text{N}_4$ , ZS is  $\text{ZrSiO}_4$ , m is monoclinic  $\text{ZrO}_2$ , t is tetragonal  $\text{ZrO}_2$ , O' is O'-sialon, s is strong, m is medium, w is weak, and v is very.

Sample	Crystalline phase present			
	$\alpha$	ZS	m	t
E1	s	s	vw	vvw
E3	s	s	vw	vvw
E4	s	s	vw	vvw

(a)

Sample	Crystalline phase present			
	$\alpha$	ZS	m	t
E1	s	s	mw	w
E3	s	s	mw	w
E4	s	s	mw	w

(b)

Sample	Crystalline phase present				
	$\alpha$	ZS	m	t	O'
E					
E1	ms	ms	ms	w	m
E3	mw	m	s	w	ms
E4	w	vw	s	w	ms

(c)

Sample	Crystalline phase present			
	$\alpha$	m	t	O'
E	mw	s	w	s
E1	—	s	w	s
E3	vvw	s	mw	s
E4	vvw	ms	m	s

(d)

Sample	Crystalline phase present			
	$\alpha$	m	t	O'
E				
E1	—	s	w	s
E2				
E3	—	s	mw	s
E4	—	ms	m	s
E5				

(e)

Sample	Crystalline phase present			
	$\alpha$	m	t	O'
E	—	s	w	s
E1	vvw	s	vw	s
E2	vvw	s	vw	s
E3	vvw	s	w	s
E4	vvw	s	mw	s
E5	—	ms	m	s

(f)

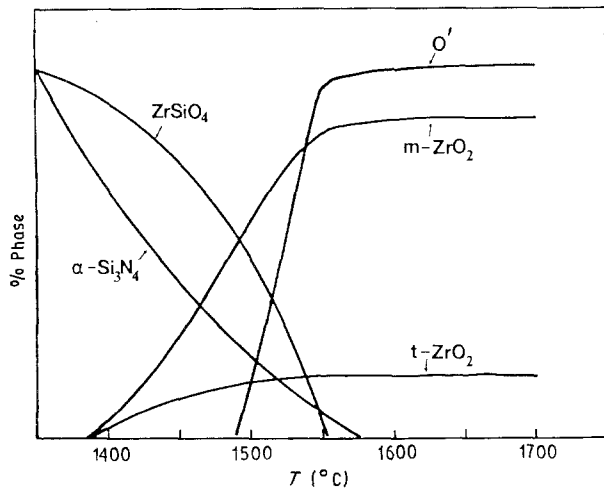


Figure 1 Reaction sequence of  $\text{Sm}_2\text{O}_3$  containing  $\text{O}'\text{-ZrO}_2$  composites after reacting for 1 h at 1300–1700 °C.

(sample E5), most of the zirconia resulting from the decomposition of zircon was in monoclinic form. Cracks were generated in the material due to the spontaneous transformation of the zirconia from tetragonal to monoclinic form on cooling (Fig. 2). This result is remarkably different from the  $\text{Y}_2\text{O}_3$ -containing system where 5.5 wt %  $\text{Y}_2\text{O}_3$  in the same composition stabilized all the zirconia into a non-transformable  $t'$  structure [2], suggesting a lower solubility of  $\text{Sm}_2\text{O}_3$  in  $\text{ZrO}_2$ . However the advantage of this effect is that a secondary additive can be selected for stabilizing the  $\text{ZrO}_2$  without interfering with the role of the densification additive, which was the original reason for exploring combined oxide additives. Pure  $\text{ZrSiO}_4$  dissociates into  $\text{ZrO}_2$  and  $\text{SiO}_2$  above 1675 °C [8]. But its dissociation temperature can be significantly reduced if there is an additional liquid in the system and in the present system this started at

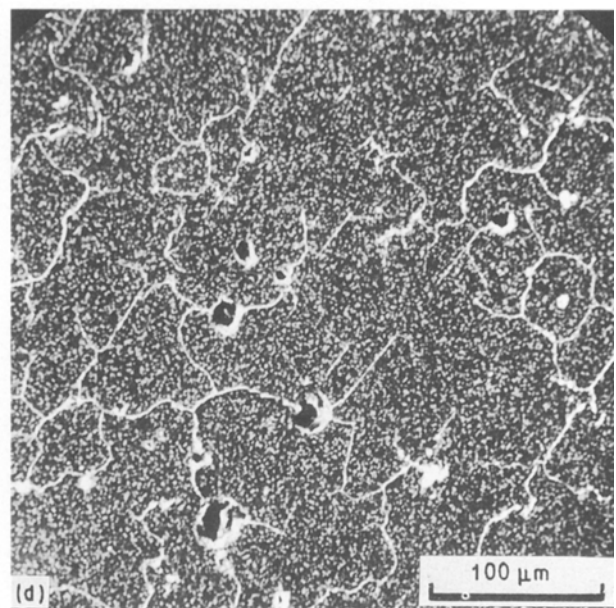
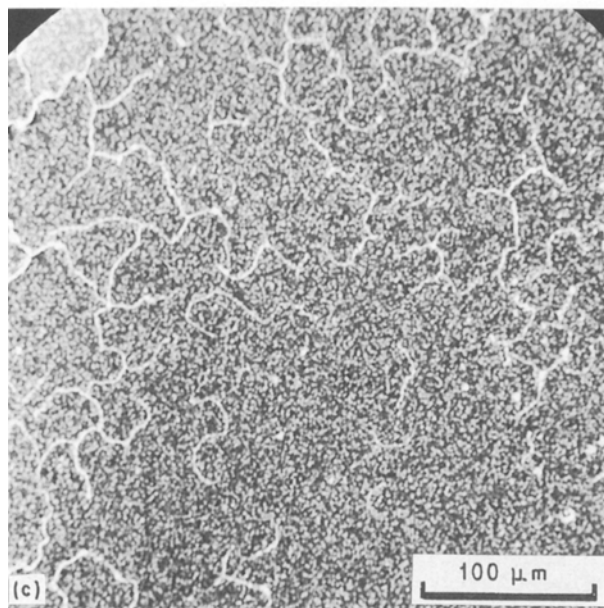
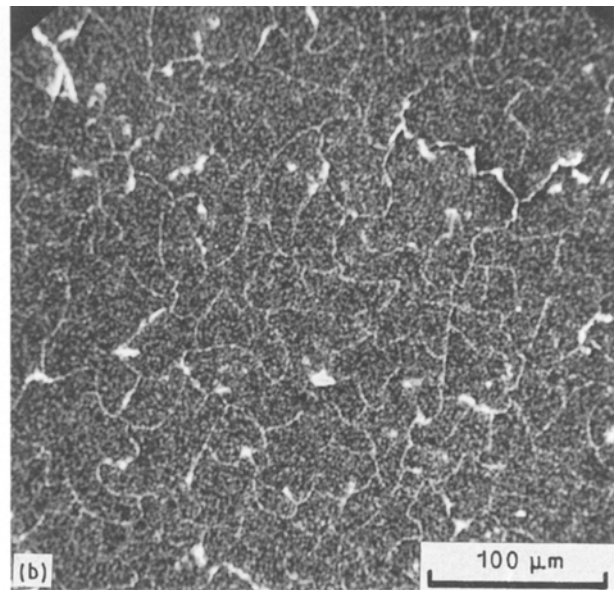
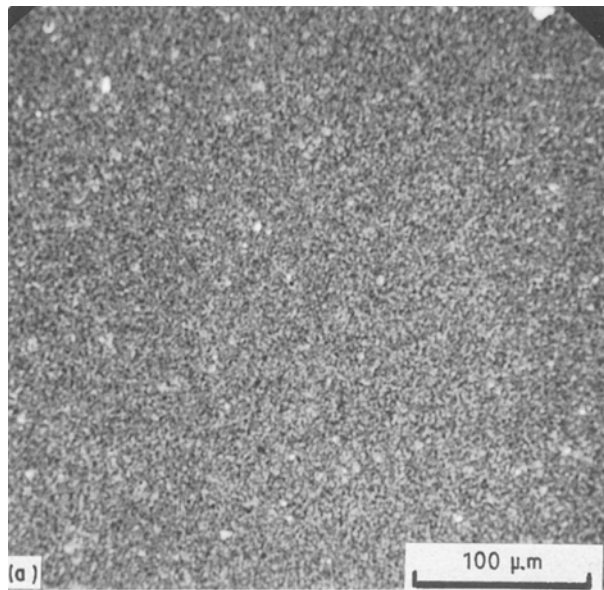


Figure 2 Microstructure of sample E3 (3 wt %  $\text{Sm}_2\text{O}_3$ ) sintered at different temperatures: (a) 1500 °C/1h, (b) 1550 °C/1h, (c) 1600 °C/1h, (d) 1700 °C/1h. Notice the microcracks in the samples sintered above 1500 °C and the large pores resulted from bloating effect at 1700 °C.

TABLE III Densities of samples sintered at different temperatures for 1 h

Sample	Density ( $\times 10^3 \text{ kg m}^{-3}$ )							
	1200°C	1300°C	1400°C	1500°C	1550°C	1600°C	1700°C	1700°C*
E					3.279		3.374	
E1		2.541	3.047	3.390	3.477	3.438	3.369	3.435
E2							3.366	
E3	2.289	2.492	3.215	3.528	3.505	3.508	3.355	3.464
E4		2.719	3.434	3.643	3.583	3.494	3.322	3.503
E5							3.161	

\* A modified sintering schedule of 1550°C for 0.5 h followed by 1700°C for 0.5 h was used.

1400°C. From the X-ray results obtained at 1500°C, it was seen that high  $\text{Sm}_2\text{O}_3$  contents resulted in less unreacted  $\text{ZrSiO}_4$  in the samples, indicating that the  $\text{Sm}_2\text{O}_3$ -containing liquid formed at approximately 1400°C and then facilitated the dissociation of  $\text{ZrSiO}_4$ .

### 3.2. Densification behaviour

Densities of materials sintered at different temperatures are given in Table III and these data can be compared with the calculated density  $3.46 \times 10^3 \text{ kg m}^{-3}$  for sample E3 (the  $\text{Sm}_2\text{O}_3$  content in the sample was ignored in the calculation). It is seen that densification of the composites starts at an early stage of sintering (about 1400°C) and the density continuously increases up to 1500°C. X-ray diffraction indicated the existence of large amounts of unreacted zircon and silicon nitride in the materials sintered below 1500°C but confirmed the disappearance of both  $\text{Al}_2\text{O}_3$  and  $\text{Sm}_2\text{O}_3$  in these samples. It was suggested that the densification of the materials at these temperatures was due to the formation of a mixture of unreacted powder and reactant joined together by a low viscosity Sm-Si-Al-O-N liquid phase. Clearly the low eutectic temperature in this system facilitates densification preceding zircon dissociation and this offers an important advantage because the final sintering temperature can then be determined by the minimum temperature at which full conversion from  $\alpha\text{-Si}_3\text{N}_4$  to  $\text{O}'\text{-sialon}$  can be achieved. At this temperature (1500–1550°C), grain growth of zirconia is minimal and this allows control of small grain size for the zirconia particles, which is a critical factor for controlling the tetragonal to monoclinic transformation. These results are very different from those found in the same material but using 2.2 wt %  $\text{Y}_2\text{O}_3$  as the additive, when the maximum densification was not obtained until 1650°C [7] (see Fig. 3).

The maximum densification of  $\text{O}'\text{-ZrO}_2$  composites was achieved between 1550 and 1600°C after the completion of the reaction between  $\text{ZrSiO}_4$  and  $\text{Si}_3\text{N}_4$ , even at  $\text{Sm}_2\text{O}_3$  contents as low as 1–3 wt % (i.e. 0.5–1.4 mol %). Whereas additions of about 4 wt % yttria to the same composition gave final densities of  $3.43 \times 10^3 \text{ kg m}^{-3}$  after sintering for 1 h at 1700°C [2], only 1 wt %  $\text{Sm}_2\text{O}_3$  is sufficient to give densities of  $3.48 \times 10^3 \text{ kg m}^{-3}$  when sintered at temperatures of

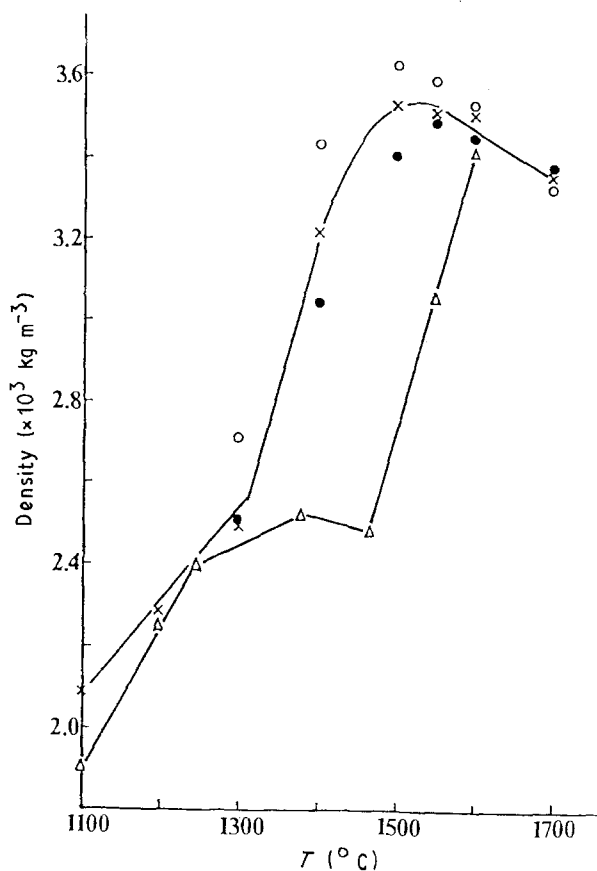


Figure 3 Densification behaviour of  $\text{Sm}_2\text{O}_3$  containing  $\text{O}'\text{-ZrO}_2$  samples and the same compositions with  $\text{Y}_2\text{O}_3$  addition. The result of the  $\text{Y}_2\text{O}_3$ -containing sample is quoted from [7]. (●) E1 1 wt %  $\text{Sm}_2\text{O}_3$ , (×) E3 3 wt %  $\text{Sm}_2\text{O}_3$ , (○) E4 6 wt %  $\text{Sm}_2\text{O}_3$ , (△) 2.2 wt %  $\text{Y}_2\text{O}_3$  [7].

1550°C. The significant discrepancy between the densities of sample E (i.e. Z-23 without any additive) and sample E1 (Z-23 plus 1 wt %  $\text{Sm}_2\text{O}_3$ ) at low sintering temperatures (e.g. 1550°C) shows the large effect produced by the introduction of a tiny amount of  $\text{Sm}_2\text{O}_3$ . On the other hand, 1700°C is too high a sintering temperature for the samples containing  $\text{Sm}_2\text{O}_3$  and bloating is observed (Fig. 2), which reduces the density (Fig. 3). Moreover it was found that increasing the  $\text{Sm}_2\text{O}_3$  level resulted in worse bloating of the samples (Table III). A modified firing cycle, with the samples held for 0.5 h at an intermediate temperature (1550°C) before the final 0.5 h at 1700°C, avoided the bloating problems to some extent; but the densities of the samples were slightly lower than those fired at

1550–1600 °C, indicating the instability of the liquid phase at high temperature.

### 3.3 Microstructures

Microcracks on the surface of the materials, induced by the transformation from tetragonal to monoclinic zirconia on cooling, were clearly observed in the samples sintered above 1550 °C, at which temperature the conversion from zircon to zirconia was complete (Fig. 2). The size of  $ZrO_2$  grains in samples sintered up to 1500 °C was less than 0.5  $\mu m$  but particle size increased significantly with increasing temperature (Fig. 4). It was realized that the  $ZrO_2$  particle size could be controlled below the 1  $\mu m$  level at 1550 °C. Above this temperature, grain growth was unavoidable unless other procedures were adopted. The polygonal morphology of the  $ZrO_2$  dispersion in the 1700 °C sintered sample clearly indicated that coales-

cence of small grains at the high temperature was one of the major factors affecting grain growth (Fig. 4d). However the grain growth of  $O'$ -sialon phase with temperature seems to be less significant than that of zirconia particles. The different orientations of needle-like  $O'$  particles might be able to prevent coalescence of  $ZrO_2$  grains even at high sintering temperatures. Therefore, reducing the zircon content of the starting mix would be helpful to depress this grain growth.

Fig. 5 shows a transmission electron micrograph of sample E3, from which an amorphous grain-boundary pocket between m- $ZrO_2$  and  $O'$  grains in the sample is clearly observed. Estimations indicated that the total glass content was about 5 vol %, which was more than expected. This glassy phase wets the  $ZrO_2$  and  $O'$  grains but some drawbacks also result. The Young's modulus is lowered and this facilitates increased grain growth of  $ZrO_2$ , which does not benefit the transformation toughening. The glassy phase will also re-

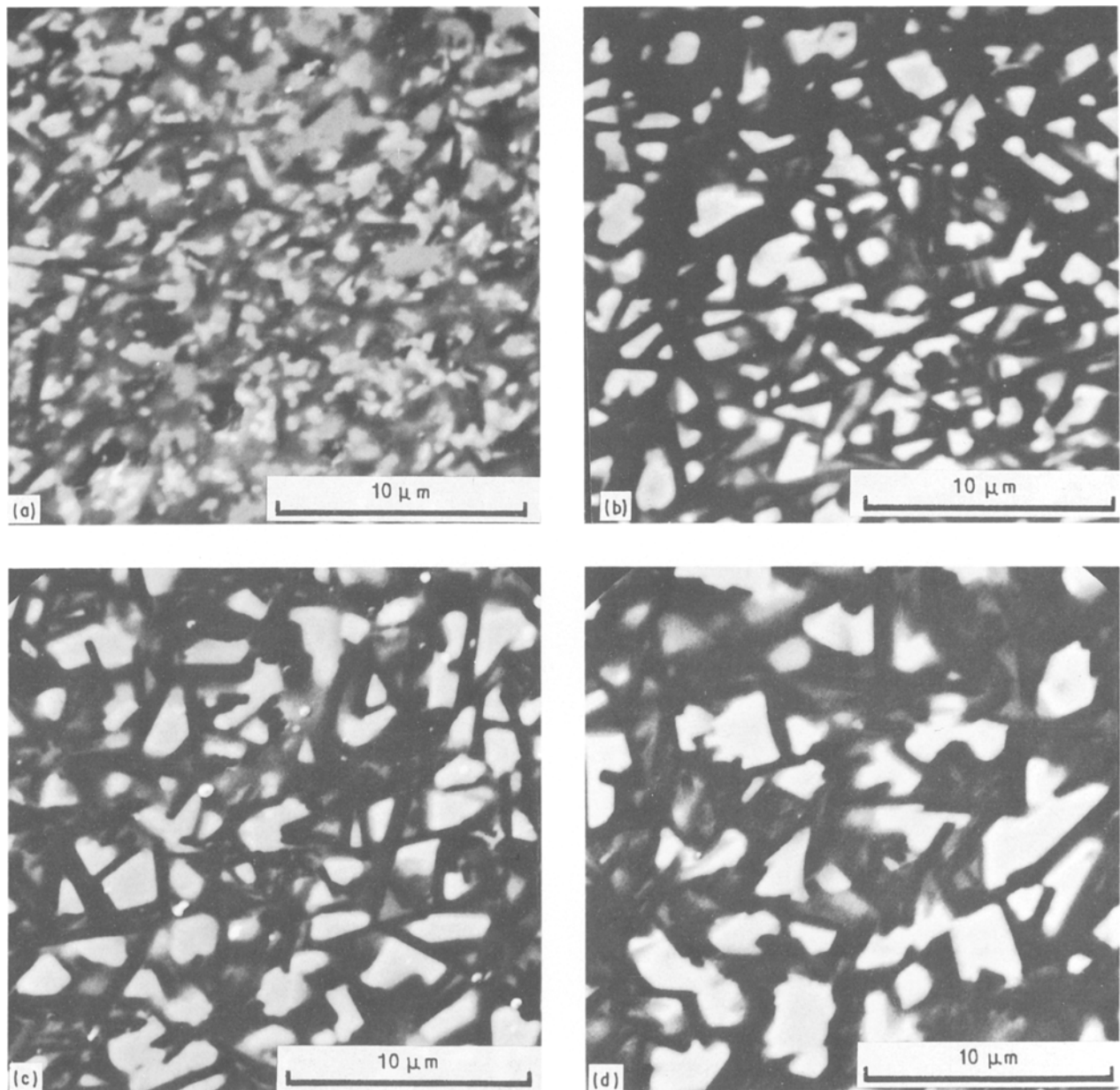


Figure 4 The variation of average  $ZrO_2$  grain size ( $D_a$ ) with sintering temperature in sample E3 (3 wt%  $Sm_2O_3$ ): (a) 1500 °C/1h,  $D_a = 0.5 \mu m$ ; (b) 1550 °C/1h,  $D_a = 0.9 \mu m$ ; (c) 1600 °C/1h,  $D_a = 1.2 \mu m$ ; (d) 1700 °C/1h,  $D_a = 2.0 \mu m$ .

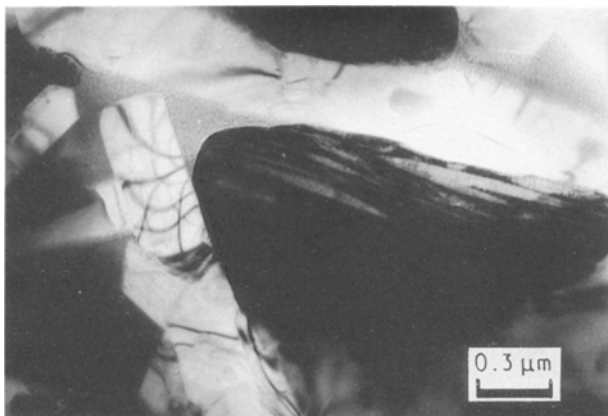


Figure 5 Transition electron micrograph of sample E3. The dark phase is m-ZrO<sub>2</sub> and the needle-like phase is O'-sialon. Notice the amorphous pocket in between ZrO<sub>2</sub> and O' phases.

tard the toughening effect by providing an easy route for crack propagation. Furthermore, this relatively soft boundary could severely degrade the high temperature properties of the material. Post heat treatment of the material at 1150 °C and 1300 °C for 24 h failed to devitrify any new grain-boundary phase from the glassy pockets, apart from a trace amount of  $\alpha$ -cristobalite and zircon at 1300 °C. Clearly the heat-treatment behaviour of the material should be further investigated.

#### 4. Conclusion

The addition of very small amounts of Sm<sub>2</sub>O<sub>3</sub> can significantly densify ZrO<sub>2</sub>-O' sialon composites at

relatively low sintering temperatures. This extraordinary densification behaviour is superior to other common additives. Sm<sub>2</sub>O<sub>3</sub> cannot effectively stabilize ZrO<sub>2</sub> and hence a secondary additive has to be used to achieve a transformable ZrO<sub>2</sub> phase in the composite.

#### Acknowledgement

The authors are most grateful for the financial support from Cookson Group PLC, UK for the period when this work was carried out.

#### References

1. R. POMPE, in "Structural ceramics - Processing, microstructure and properties", edited by J. J. Bentzen, J. B. Bilde-Sorensen, N. Christiansen, A. Horsewell and B. Ralph (Riso National Laboratory, 1990), p. 97.
2. Y. CHENG, D. P. THOMPSON and S. SLASOR, "Ceramics-adding the value", Proceedings of Austceram '92, edited by M. J. Bannisters (CSIRO, 1992) p. 504.
3. Y. CHENG and D. P. THOMPSON, *Proc. Brit. Ceram. Soc.* **42** (1988) 149.
4. R. STEVENS, "Zirconia and zirconia ceramics", (Magnesium Elektron Ltd, London 1986) No. 113.
5. A. G. EVANS and E. A. CHARLES, *J. Am. Ceram. Soc.* **59** (1976) 371.
6. M. B. TRIGG and K. H. JACK, in "Ceramic components for engines", edited by S. Somiya, E. Karai and K. Ando, (KTK Scientific, Tokyo, 1983) p. 199.
7. S. W. THOMPSON, "Internal Progress Report", Cookson Group, 1987.
8. W. C. BUTTERMAN and W. R. FOSTER, *Amer. Mineral.* **53** (1967) 880.

Received 11 August 1992

and accepted 14 September 1992